Syntheses, Structures, and Optical Properties of β-Ferrocenylacrylate Metal Polymers

Lin Ke Li,[a] Ying Lin Song,[b] Hong Wei Hou,*[a] Yao Ting Fan,[a] and Yu Zhu[a]

Keywords: Cadmium / Lead / Nonlinear optics / Organic–inorganic hybrid composites / Polymers

The zero-dimensional polymer $[Pb_6(\mu_2OOCCH{=}CHFc)_2(\mu_3\text{-}OOCCH{=}CHFc)_2(\mu_2\text{-}\eta^2\text{-}OOCCH{=}CHFc)_2(\eta^2\text{-}OOCCH{=}CHFc)_2(\mu_4\text{-}O)_2]$ (**1**), the one-dimensional chain polymers $[Pb(\eta^1\text{-}\mu_2\text{-}OOCCH{=}CHFc)_2(phen)]_n$ (phen = phenanthroline; (**2**), $\{[Cd(\mu_2\text{-}\eta^2\text{-}OOCCH{=}CHFc)(\eta^2\text{-}OOCCH{=}CHFc)(H_2O)_2](H_2O)_4\}_n$ (**3**), and the two-dimensional hybrid polymer $\{[Cd(\eta^2\text{-}OOCCH{=}CHFc)(bbbm)_{1.5}Cl]\cdot 1.5H_2O\}_n$ [bbbm = 1,1′-(1,4-butanediyl)bis-1*H*-benzimidazole; **4**] have been prepared by the reaction of sodium β-ferrocenylacrylate [FcCH=CHCOONa, Fc = $(\eta^5\text{-}C_5H_5)Fe(\eta^5\text{-}C_5H_4)$] with the appropriate metal salts. Solution-state differential pulse voltammetry for **1**–**4** indicated that the half-wave potentials of the ferrocenyl moieties in these polymers are all shifted to positive potential compared with that of sodium β-ferrocenylacrylate. The four polymers' third-order nonlinear optical (NLO) properties were determined by the Z-scan technique in DMF solutions. The results show that these polymers possess good nonlinear optical refraction effects. Their hyperpolarizability (γ) values are calculated to be 4.80×10^{-30}, 5.19×10^{-30}, 1.57×10^{-29}, and 2.04×10^{-29} esu for **1**–**4**, respectively. The γ values of the Cd^{II} polymers (**3** and **4**) are slightly larger than those of the Pb^{II} polymers (**1** and **2**), which indicates that the metal ions play an important role in the NLO properties of these polymers.

Introduction

Currently, the rational design and synthesis of metal–organic polymeric complexes containing multifunctional groups have received much attention because of their widespread potential applications in molecular sensor technology, peptide mimetic models, charge-transfer complexes, non-linear optical materials, organic synthesis, homogeneous catalysis, materials chemistry, and so on.[1–5] Due to the fascinating properties of the ferrocene moiety as well as the versatile coordination modes[6] and strong coordinating capability of the carboxylate groups, ferrocenecarboxylate compounds have been extensively used as functional ligands.[7–14] Furthermore, the introduction of ferrocenyl carboxylate groups into metal–organic frameworks provides an effective way to prepare new functional materials with unique features.

Ferrocenecarboxylate and ferrocenedicarboxylate were among the first to be prepared and studied in synthetic strategies, and lots of metal-based polymers containing them have been described.[12,13,15–20] However, relatively few reports have appeared on other ferrocenecarboxylate–metal polymers. In recent years, various groups and ourselves have put effort into the synthesis and property investigations of other ferrocenecarboxylate–metal polymers,[10,11] such as the structures and the redox properties of the polymers $[Pb(o\text{-}OOCC_6H_4COFc)(\eta^2\text{-}o\text{-}OOCC_6H_4COFc)(bpe)]_n$, $\{[Zn(o\text{-}OOCC_6H_4COFc)_2(4,4'\text{-}bpy)(H_2O)_2]\cdot 2MeOH\cdot 2H_2O\}_n$, $\{[Cd(o\text{-}OOCC_6H_4COFc)_2(bpe)(MeOH)_2]\cdot 2H_2O\}_n$, $\{[Pb\{\mu_2\text{-}\eta^2\text{-}OOCCH{=}(CH_3)CFc\}_2]\cdot MeOH\}_m$,[10] and $\{[Cd(\mu_2\text{-}OOCH_4C_6Fc)(\eta^2\text{-}OOCH_4C_6Fc)(bbp)](CH_3OH)\}_n$,[11] and the magnetic properties of $\{[Mn(OOCH_4C_6Fc)_2(\mu_2\text{-}OH_2)(H_2O)_2](H_2O)\}_n$ and $[Mn(\mu_2\text{-}OOCH_4C_6Fc)_2(phen)]_n$,[11] etc., but no reports have touched on the third-order NLO properties of ferrocenecarboxylate–metal polymers.

Following our earlier studies on ferrocenecarboxylate–metal polymers, we report here the syntheses and structures of a series of novel polymers constructed from FcCH=CHCOONa with Pb^{II} or Cd^{II} ions and subsidiary ligands. The third-order NLO studies in DMF solution show that all these polymers display self-focusing behaviors. This result is consistent with the previous conclusion that the NLO properties of coordination polymers are controlled by the valence shell structures of the central metal ions. Their thermal and electrochemical properties were also investigated.

Results and Discussion

Preparation of the Polymers

Polymers **1**–**4** were obtained by treatment of FcCH=CHCOONa with the appropriate metal salts and subsidiary

[a] Department of Chemistry, Zhengzhou University, Henan 450052, P. R. China
Fax: +86-371-7761744
E-mail: houhongw@zzu.edu.cn
[b] Department of Applied Physics, Harbin Institute of Technology, Heilongjiang 150001, P. R. China

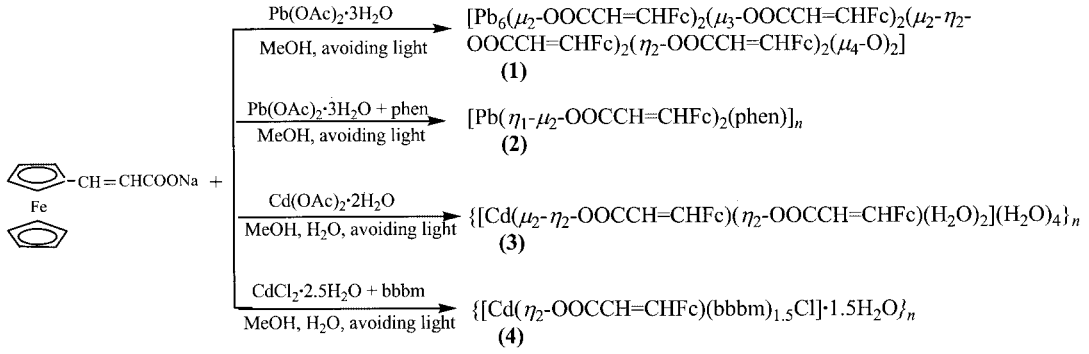

Scheme 1.

ligands in different solvents (Scheme 1). Crystals suitable for X-ray crystallography of polymers **1**–**4** were also obtained by slow evaporation of the solvents in the dark due to the reasons mentioned previously.[21] These crystals are only soluble in highly polar solvents such as DMSO and DMF, etc.

Under similar reaction conditions, the reactions of $Pb(OAc)_2$ with different ferrocenecarboxylates generate different structural geometries. For example, treatment of $Pb(OAc)_2$ with FcCOONa or $FcC(CH_3)$=CHCOONa gives the one-dimensional chain structural polymers $\{[Pb_2(OOCFc)(\eta^2\text{-}OOCFc)(\mu_2\text{-}\eta^2\text{-}OOCFc)(\mu_3\text{-}\eta^2\text{-}OOCFc)(MeOH)]\cdot 1.5MeOH\cdot H_2O\}_n$[6e] or $\{[Pb\{\mu_2\text{-}\eta^2\text{-}OOCCH=(CH_3)CFc\}_2]\cdot MeOH\}_n$,[10] while when FcCH=CHCOONa was treated with $Pb(OAc)_2$ a zero-dimensional polymer (**1**) was obtained whose structure displays significant difference from the former two polymers. The addition of phen to the reaction system of **1** led to the formation of the one-dimensional polymer **2**. Up to now, the synthesis of two-dimensional polymers containing ferrocenecarboxylate was still a great challenge. On the basis of self-assembly of coordination polymers, we successfully prepared a novel, two-dimensional hybrid polymer **4** with the organic bridging ligand bbbm.

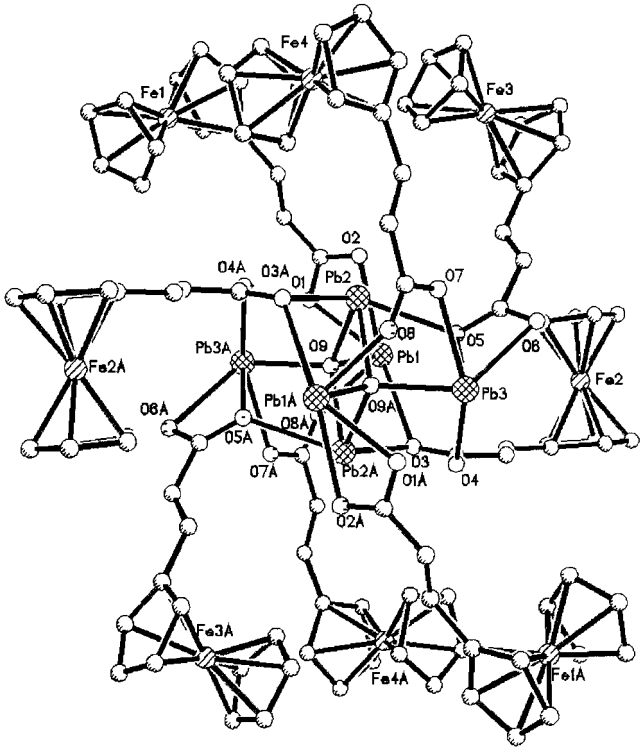

Figure 1. Crystal structure of $[Pb_6(\mu_2\text{-}OOCCH=CHFc)_2(\mu_3\text{-}OOCCH=CHFc)_2(\mu_2\text{-}\eta^2\text{-}OOCCH=CHFc)_2(\eta^2\text{-}OOCCH=CHFc)_2(\mu_4\text{-}O)_2]$ (**1**) with heteroatom labeling scheme.

Crystal Structure of $[Pb_6(\mu_2\text{-}OOCCH=CHFc)_2(\mu_3\text{-}OOCCH=CHFc)_2(\mu_2\text{-}\eta^2\text{-}OOCCH=CHFc)_2(\eta^2\text{-}OOCCH=CHFc)_2(\mu_4\text{-}O)_2]$ (1)

The molecule crystallizes in the space group $P\bar{1}$. X-ray diffraction analysis revealed that **1** is a zero-dimensional Pb^{II} polymer (Figure 1). The structure shows a giant, scroll-wheel-like arrangement of the eight ferrocene units in four kinds of coordination modes with a presumed Pb_6 octahedron core (the six Pb^{II} ions inhabit the six apexes of the presumed octahedron), and the six Pb^{II} ions are bridged by two $\mu_4\text{-}O^{2-}$ anions from the inner of the Pb_6 octahedron core, simultaneously. The molecule sits astride a center of inversion.

The eight $FcCH=CHCOO^-$ units surround the Pb_6 core and bridge the six Pb^{II} ions to form a stable Pb_6 octahedron. It is interesting that the eight $FcCH=CHCOO^-$ units display four kinds of coordination modes: bidentate (η^2-OOCCH=CHFc), bidentate (μ_2-OOCCH=CHFc), tridentate (μ_3-OOCCH=CHFc), and tridentate ($\mu_2\text{-}\eta^2$-OOCCH=CHFc). As for the Pb_6 octahedron, the mean deviation of the plane Pb2–Pb2A–Pb3–Pb3A (**A**), Pb1–Pb1A–Pb2–Pb2A (**B**), or Pb1–Pb1A–Pb3–Pb3A (**C**) is 0.000 Å. The dihedral angle between planes **A** and **B** is 68.8°, that between **A** and **C** is 85.5°, and that between **B** and **C** is 85.8°. The Pb1–Pb1A, Pb2–Pb2A, and Pb3–Pb3A distances are 6.621, 3.725, and 6.546 Å, respectively.

The six Pb^{II} ions lie in three kinds of coordination environments, considering an arbitrary length of approximately 2.8 Å to define maximum bonding interactions (this being the sum of the two ionic radii[22]). Pb1 and Pb3 are pentacoordinate. Each Pb1 binds to five oxygen atoms, two from a chelating η^2-OOCCH=CHFc$^-$ unit, one from bidentate μ_2-OOCCH=CHFc$^-$, one from tridentate μ_3-OOCCH=CHFc$^-$, and one from the μ_4-O^{2-} anion from the inner core of the Pb_6 octahedron. For Pb3, the five oxygen atoms are two from μ_2-η^2-OOCCH=CHFc$^-$, one from μ_3-OOCCH=CHFc$^-$, one from μ_2-OOCCH=CHFc$^-$, and one from the μ_4-O^{2-} anion. The coordination number of Pb2 is four, with four oxygen atoms from μ_2-η^2-OOCCH=CHFc$^-$, μ_3-OOCCH=CHFc$^-$, and two μ_4-O^{2-} anions. The Pb–O distances are in the range 2.264(8)–2.694 Å. This contrasts with the Pb atoms in the acetate, formate, and pentafluorobenozate complexes, where eightfold coordination is found;[23] coordination numbers of 7,[24] 9,[25] and 10[26] are also known in other Pb^{II} carboxylates.

The eight ferrocene fragments are located around the Pb_6 octahedron. Fe1, Fe4, Fe1A, and Fe4A are co-planar, as are Fe2, Fe3, Fe2A, and Fe3A, and the dihedral angle between the two planes is 89.8°, that is to say they are nearly perpendicular to each other.

It has previously been reported that bridging oxygen atoms are present at the center of a polyhedron formed by transition[27] and main- group[28] metals or hetero-polymetal containing Pb atoms,[29] for example the zero-dimensional Zn^{II} polymers $[(Zn_4O)(O_2CR)_6]$ (R = diethylamino, piperidino, or pyrrolidino),[30] and $[Zn_4(\mu_2\text{-}FcCOO)_6(\mu_4\text{-}O)]$.[6e] Reports on Pb^{II} carboxylate complexes containing an oxide ligand bridging the metal atoms in a homometallic polyhedron of Pb^{II} ions are very scare.[23]

Crystal Structure of $[Pb(\eta^1\text{-}\mu_2\text{-}OOCCH=CHFc)_2(phen)]_n$ (2)

The 1D chain structure of polymer **2** is formed by a double monatomic bridge connecting the adjacent Pb^{II} ions (Figure 2). Each Pb^{II} ion adopts a distorted octahedral PbN_2O_4 coordination environment. The repeated Pb_2O_2 rings construct the basic skeleton structure of the one-dimensional chain: the dimensions of the rhomboid are 2.549×2.734 Å^2, the dihedral angle between the two adjacent Pb_2O_2 rhomboid is 81.8°, and the Pb···Pb intrachain distance is 4.202 Å. The phen rings lie on alternate sides of each chain, parallel to the *c*-axis. The $Pb–N_{(phen)}$ distance [2.612(11) Å] is consistent with those in $\{[Pb(phen)_2(ox)]\cdot 5H_2O\}_n$ (ox = oxalate) [2.721(2) Å],[31] $[Pb(phen)(O_2CCH_3)(O_2NO)]_n$ [2.519(3) and 2.579(3) Å],[32] $[Pb(phen)_2(O_2CCH_3)(ClO_4)]$, and $[Pb(phen)_2(O_2CCH_3)(NCS)]_2$,[32] etc.

The Pb_2O_2 ring in **2** is different from those in dimeric $[Pb(phen)(O_2CCH_3)_2]_2$[33] and $[Pb(phen)(O_2CCH_3)(NCS)]_2$[34] and polymeric $[Pb(phen)(O_2CCH_3)(O_2ClO_2)]_n$[35] and $[Pb(phen)(O_2CCH_3)(O_2NO)]_n$,[36] where the Pb_2O_2 rings share edges with PbOCO quadrilaterals to form the dimer core. The long edge of the Pb_2O_2 ring in **2** (2.734 Å) is similar in length to those in $[Pb(phen)(O_2CCH_3)(O_2NO)]_n$ (2.80 Å) and $[Pb(phen)(O_2CCH_3)(O_2ClO_2)]_n$ (2.74 Å), but considerably shorter than those in $[Pb(phen)(O_2CCH_3)(NCS)]_2$ (3.19 Å) and $[Pb(phen)(O_2CCH_3)_2]_2$

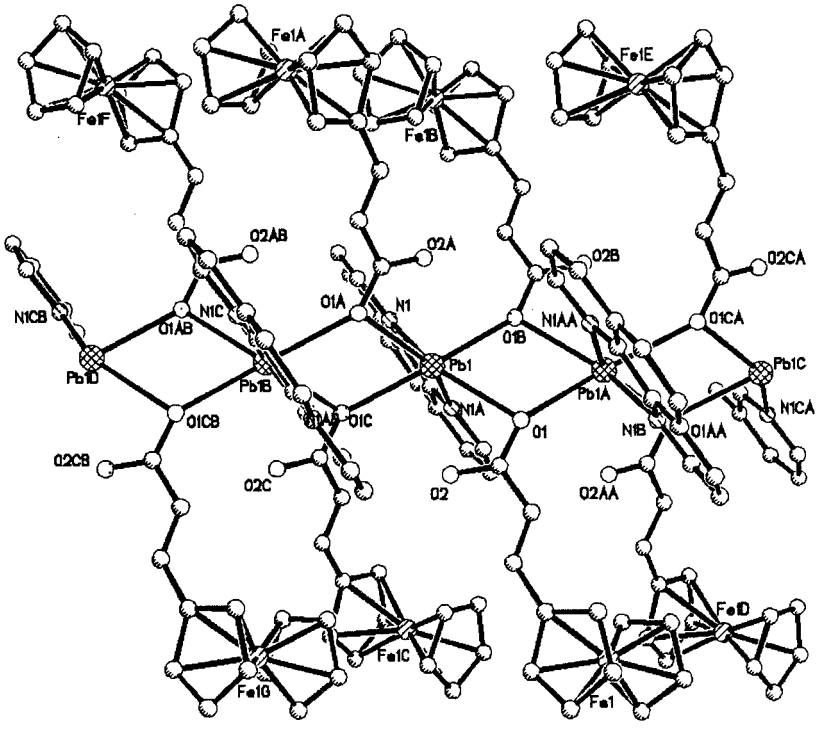

Figure 2. Perspective view of the 1D chain structure of $[Pb(\eta^1\text{-}\mu_2\text{-}OOCCH=CHFc)_2(phen)]_n$ (**2**) with only the heteroatoms labeled.

(3.37 Å). This indicates the strong coordinating ability of the FcCH=CHCOO$^-$ anion.

Since the distance between adjacent phen rings (8.270 Å) on one side of the 1D chain is out of the range of π–π stacking interactions there are no such interactions in the crystal structure, and it is the intermolecular interaction that is responsible for the packing in the solid-state structure.

Crystal Structure of {[Cd(μ$_2$-η^2-OOCCH=CHFc)-(η^2-OOCCH=CHFc)(H$_2$O)$_2$](H$_2$O)$_4$}$_n$ (3)

The X-ray diffraction analysis revealed that **3** crystallizes in the space group $P2_1/n$. As can be seen from Figure 3, each Cd^{II} ion is seven-coordinate and the adjacent [Cd(η^2-OOCCH=CHFc)(H$_2$O)$_2$] groups are linked by μ$_2$-η^2-OOCCH=CHFc$^-$ units into a one-dimensional chain polymer.

In the structural unit, each Cd^{II} ion binds to atoms O1 and O2 from a chelating η^2-OOCCH=CHFc$^-$, O3, O4, and O4A atoms from two μ$_2$-η^2-OOCCH=CHFc$^-$, groups and the O5 and O6 atoms from two coordinated H$_2$O molecules. The Cd–O$_{(OOCCH=CHFc^-)}$ distances are in the range 2.242(4)–2.580(5) Å. The Cd^{II} ions are not in a straight line: the adjacent Cd···Cd separation is 4.637 Å and the Cd–Cd–Cd angle is 105.5°. The one-dimensional [Cd(μ$_2$-η^2-OOCCH=CHFc)(η^2-OOCCH=CHFc)(H$_2$O)$_2$] chain extends along the *b*-direction. Viewed along the *b*-axis, two kinds of ferrocene fragments are located along both sides of the one-dimensional chain, and they alternate along this chain. The one-dimensional chains are connected by O–H···O hydrogen bonds and intermolecular interactions (Figure 4). The structure is similar to the reported 1-D infinite zigzag chain polymer [Cd{Fc(CO$_2$)$_2$}(DMF)$_2$(H$_2$O)]$_n$,[19] in which the Cd^{II} atoms are connected by the 1,1′-ferrocenedicarboxylate ligand in a 1,3′-disubstituted bridging mode.

Crystal Structure of {[Cd(η^2-OOCCH=CHFc)-(bbbm)$_{1.5}$Cl]·1.5H$_2$O}$_n$ (4)

The crystal structure analysis demonstrates that **4** crystallizes in the space group $P\bar{1}$. As shown in the structural unit (Figure 5), each Cd^{II} ion is six-coordinate in a slightly distorted octahedral environment with two oxygen atoms from a chelating η^2-OOCCH=CHFc$^-$ unit, three nitrogen atoms from three bridging bbbm ligands, and one Cl atom. The O1, O2, N3, Cl1, and Cd1 atoms are nearly co-planar (the mean deviation from the ideal CdCNO$_2$ plane is 0.0322 Å), and define the equatorial plane [Cd1–O1 = 2.273(12), Cd1–O2 = 2.476(12) Å, Cd1–N3 = 2.301(14) Å, and Cd1–Cl1 = 2.506(4) Å]. The N1 and N5 atoms of the other two bbbm units occupy the axial positions [Cd1–N1 = 2.520(13), Cd1–N5 = 2.347(12) Å], and the axial angle N1–Cd1–N5 is 166.3(4)°. All the Cd^{II} ions are bridged by the bbbm with ferrocene units in the side chain leading to an infinite two-dimensional network (Figure 6). The sheet extends along the [010] crystallographic plane.

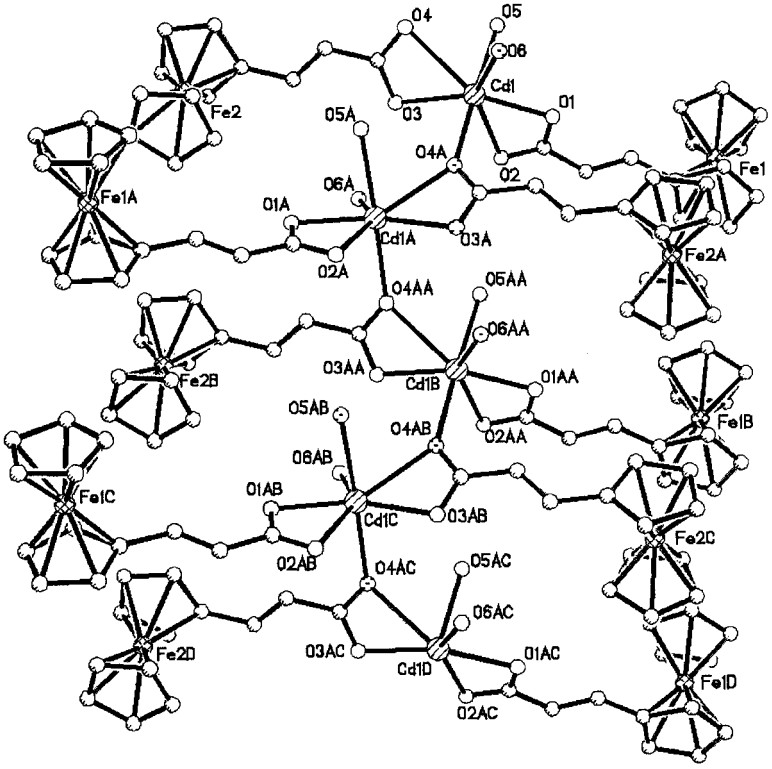

Figure 3. One-dimensional chain structure of {[Cd(μ$_2$-η^2-OOCCH=CHFc)(η^2-OOCCH=CHFc) (H$_2$O)$_2$](H$_2$O)$_4$}$_n$ (**3**) with only heteroatoms labeled.

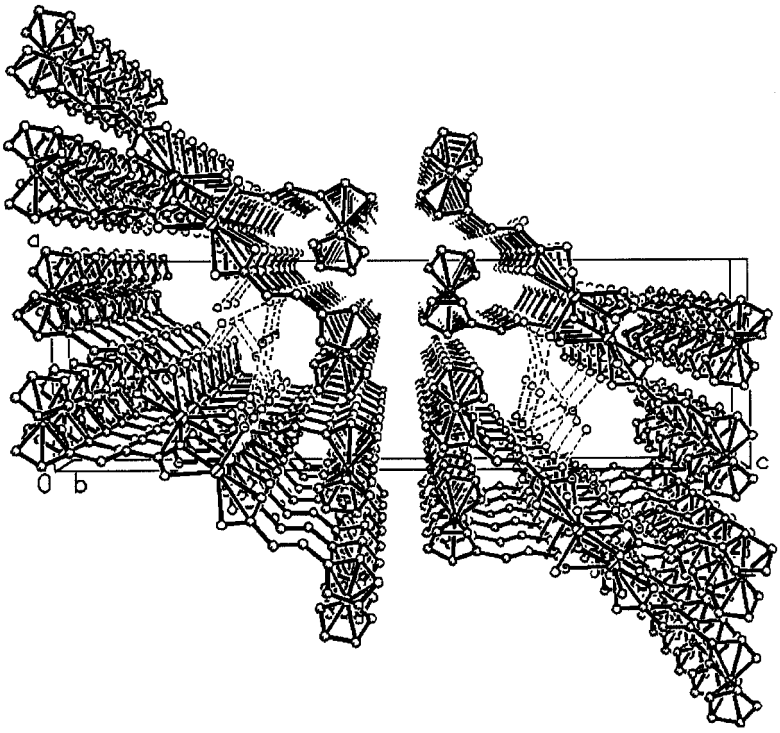

Figure 4. The solid-state structure of $\{[Cd(\mu_2\text{-}\eta^2\text{-}OOCCH{=}CHFc)(\eta^2\text{-}OOCCH{=}CHFc)(H_2O)_2](H_2O)_4\}_n$ (**3**).

Hybrid polymers with ferrocene units in the side chain have been published in our recent papers,[6e,10,11] such as the one-dimensional, ladder-like polymers $\{[Zn(OOCFc)_2(bpt)]\cdot 2.5H_2O\}_n$, $[Zn(OOCFc)(\eta^2\text{-}OOCFc)(bbp)]_n$, and $\{[Cd(\mu_2\text{-}OOCH_4C_6Fc)(\eta^2\text{-}OOCH_4C_6Fc)(bbp)](CH_3OH)\}_n$, the zigzag chain polymer $[Pb(FcCOO)(\mu_2\text{-}FcCOO)(bpe)]_n$, and the linear chain polymer $\{[Zn(o\text{-}OOCC_6H_4COFc)_2(4,4'\text{-}bpy)(H_2O)_2]\cdot 2MeOH\cdot 2H_2O\}_n$. However, two-dimensional ferrocenecarboxylate-containing hybrid polymers have not been reported up to now. Using the organic bridging ligand bbbm, we have successfully prepared the novel two-dimensional hybrid polymer **4** containing a ferrocenearboxylate component.

Thermogravimetric Analysis

The TG-DTA data of **1**–**4** were determined in the range 25–900 °C in air. It can be seen from the TG curve that **1** begins to lose weight at 212 °C, and the process of weight

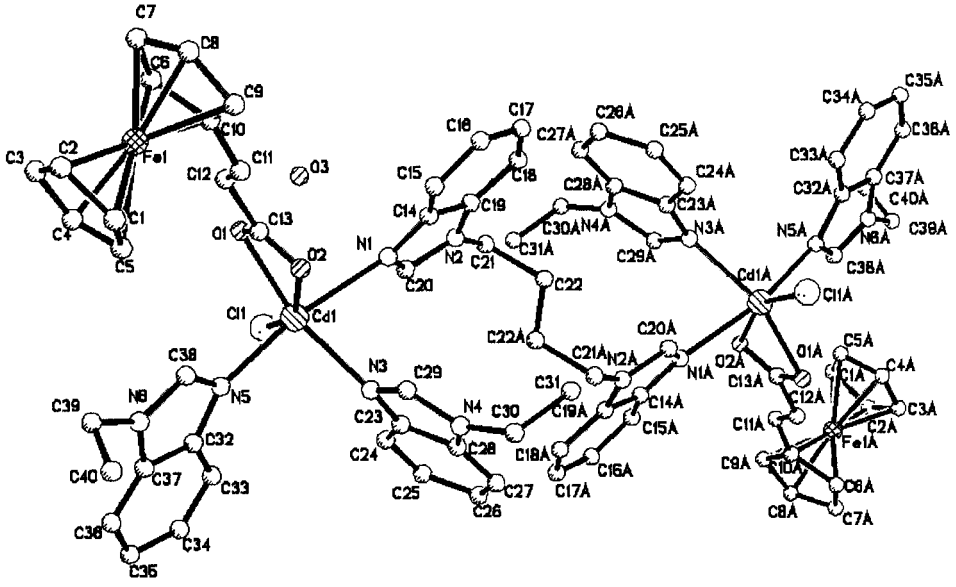

Figure 5. ORTEP diagram showing the structure unit of $\{[Cd(\eta^2\text{-}OOCCH{=}CHFc)(bbbm)_{1.5}Cl]\cdot 1.5H_2O\}_n$ (**4**). H atoms have been omitted for clarity.

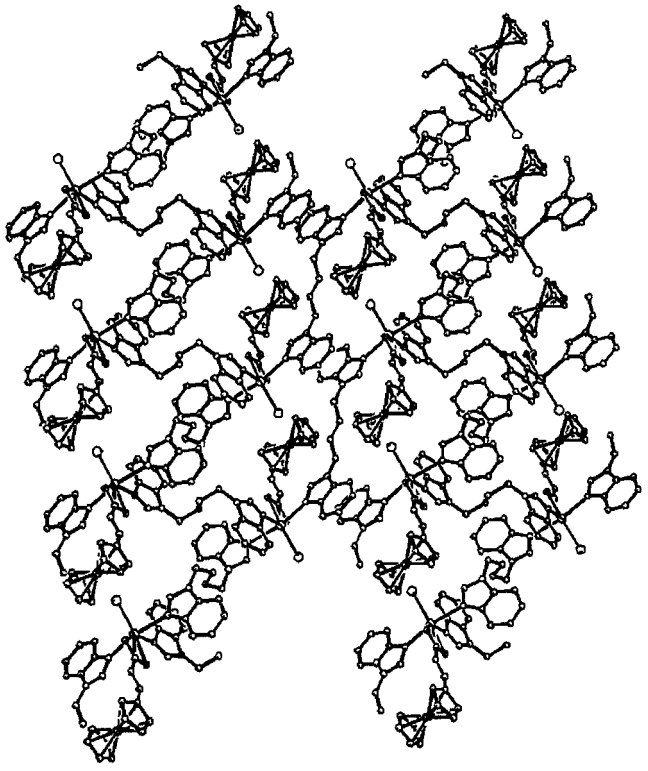

Figure 6. Two-dimensional sheet structure of $\{[Cd(\eta^2\text{-}OOCCH{=}CHFc)(bbbm)_{1.5}Cl]\cdot 1.5H_2O\}_n$ (**4**). H atoms have been omitted for clarity.

loss is sustained up to 381 °C; this corresponds to the decomposition of the FcCH=CHCOO⁻ anions. A plateau region is then observed from 381 to 900 °C. Finally, a brown amorphous residue was left, which can be assigned to 1.5PbO + 2FeO. There are two weak exothermic peaks at 258 and 304 °C, and a very strong exothermic peak at 399 °C on the DTA curve of **1**.

For polymer **2**, the weight-loss process begins at 183 °C and it goes through multiple weight loss steps, which can be assigned to the loss of the phen molecule and the decomposition of FcCH=CHCOO⁻ anions; this process is sustained up to 411 °C. A clear plateau region is then observed from 411 to 900 °C in the TGA plot. Finally, the brown amorphous residue is presumed to be PbO + 2FeO. There is one weak exothermic peak at 249 °C and one very strong exothermic peak at 390 °C on the DTA curve of **2**.

We find from the TG curve that **3** begins to lose weight at 35 °C, and this process is maintained up to 159 °C, corresponding to the loss of uncoordinated H_2O molecules. After a plateau region from 159 to 225 °C in the TG curve, it goes through complicated multiple weight-loss steps from 225 to 555 °C, corresponding to the loss of coordinated H_2O and the decomposition of the FcCH=CHCOO⁻ units. There is then a plateau region from 555 to 900 °C. The brown residue can be assigned to the residual CdO + 2FeO. There is one middle exothermic peak at 280 °C and one very strong exothermic peak at 414 °C on the DTA curve.

In the TG curve of **4**, the weight loss process from 164 to 232 °C can be assigned to the loss of H_2O molecules, then it goes through complicated multiple weight-loss steps in the temperature range of 232 to 600 °C, which can be assigned to the decomposition of bbbm and the FcCH=CHCOO⁻ anions. The final brown residue corresponds to CdO + FeO. The weight remains constant from 600 to 900 °C. In the DTA curve of **4**, there is a weak exothermic peak at 260 °C, a middle exothermic peak at 395 °C, and a very strong exothermic peak at 478 °C.

Redox Properties

The solution-state differential pulse voltammograms of **1**–**4** and FcCH=CHCOONa are shown in Figure 7. It can be seen from this figure that all these polymers show a single peak with a half-wave potential ($E_{1/2}$ vs. SCE) at 0.56 V for **1**, 0.54 V for **2**, 0.53 V for **3**, and 0.52 V for **4**, which can be assigned to the electron-transfer process of the ferrocenyl moiety. Relative to free FcCH=CHCOONa (0.51 V), the half-wave potentials of **1**–**4** are all shifted to slightly higher potential. It is apparent that these shifts can be attributed to the influence of the central metal ions, and this is consistent with the previous results of transition metal–ferrocenyl systems.[9,37] The reason for this is that the conjugated π-electron systems between the two metals allow communication,[38] and the electron-withdrawing nature of the coordinated metal centers makes the ferrocene unit harder to oxidize.[39]

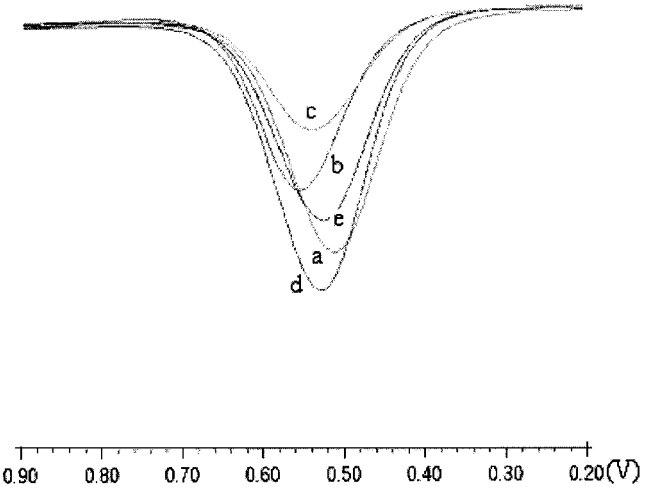

Figure 7. Differential pulse voltammogram of (a) NaOOCCH=CHFc (0.51 V), (b) **1** (0.56 V), (c) **2** (0.54 V), (d) **3** (0.53 V), (e) **4** (0.52 V) all at concentrations of approximately 1.0×10^{-3} M in DMF containing nBu$_4$NClO$_4$ (0.1 M) at a scanning rate of 20 mV s^{-1} (vs. SCE).

Nonlinear Optical Properties

The second-order NLO properties of ferrocenyl derivatives have been extensively studied,[40] but reports on the third-order NLO properties of ferrocenyl derivatives, especially ferrocenecarboxylate polymers, are very limited.

The UV/Vis spectra of **1**–**4** were determined in DMF solutions. From a previous study,[41,42] we know that ferrocene exhibits two characteristic absorptions in the UV/Vis spectra at 440 nm (assigned to the $^1E_{1g} \leftarrow {}^1A_{1g}$ transition) and 325 nm (assigned to the $^1E_{2g} \leftarrow {}^1A_{1g}$ transition). Similarly, the four polymers also show two characteristic bands at around 315 and 445 nm (Figure 8). All four polymers have a relatively low linear absorption ranging from 500 to 1000 nm, similar to other known organic–metal polymers.[42] This indicates low intensity loss and little temperature change caused by photon absorption when light propagates in the materials.

The NLO properties of **1**–**4** were investigated with a 532-nm laser pulse for 8 ns in a 1.21×10^{-4} M (**1**), 1.12×10^{-4} M (**2**), 1.37×10^{-4} M (**3**), or 1.16×10^{-4} M (**4**) DMF solution.

Figures 9a–d depict the Z-scan data for **1**–**4**, respectively. We find that all these polymers possess good nonlinear optical refraction effects. It is obvious that the theoretical curves (solid curves) reproduce well the general pattern of the observed experimental data (black dot). This fact suggests that the experimentally obtained NLO effects are effectively third-order in nature. The data show that these polymers have the same positive sign for the refractive nonlinearity, which gives rise to self-focusing behavior.

The NLO refractive effects were assessed by dividing the normalized Z-scan data obtained in the closed-aperture configuration by the normalized Z-scan data obtained in the open-aperture configuration.

The third-order NLO refractive index, n_2, can be derived from Equations (1), (2), and (3)[43]

$$T(Z,S)=\frac{\int_{-\infty}^{+\infty}\varepsilon_0 cn_0\pi\int_0^r|E_a(r,t,z)|^2 r\,dr\,dt}{S\int_{-\infty}^{+\infty}\frac{I_0\pi\omega_0^2}{2}e^{-(t/t_0)^2}dt} \quad (1)$$

$$E_a(r,t,z)=\frac{2\pi}{i\lambda(l-z)}e^{[i\pi r^2/\lambda(l-z)]}\int_0^\infty E(r',t,z)J_0\frac{2\pi r'r}{\lambda(l-z)}e^{[i\pi r'^2/\lambda(l-z)]}r'dr \quad (2)$$

$$E(r',t,z)=2\sqrt{\frac{I(r',t,z)}{\varepsilon_0 cn_0}}e^{\{(kn_2/\alpha_2)\ln[1+q(r',t,z)]\}} \quad (3)$$

where Z is the distance of the sample from the focal point, ε_0 and c are the permittivity and speed of light in vacuo, respectively, n_0 and n_2 are the linear and nonlinear refractive indices of the sample, respectively, r is the radial coordinate, t is the time, t_0 is the pulse width, I_0 is the peak irradiation intensity at focus, and $Z_0 = \pi\omega_0^2/\lambda$, with ω_0 being the spot radius of the laser beam at focus and λ being the wavelength of the laser; l is the distance between the aperture and focus, α_2 is the nonlinear absorption coefficient, and $S = 1 - \exp[-2(r_a/\omega_a)^2]$ is the linear aperture transmittance.

Based on Equation (1), the refractive index, n_2, was calculated to be 1.43×10^{-18} m^{2}W^{-1} for **1**, 1.43×10^{-18} m^{2}W^{-1} for **2**, 1.59×10^{-18} m^{2}W^{-1} for **3**, and 1.75×10^{-18} m^{2}W^{-1} for **4**. In accordance with the n_2 values, the effective third-order susceptibility $\chi^{(3)}$ can be calculated by $|\chi^{(3)}| = cn_o^2n_2/80\pi$; the $\chi^{(3)}$ values of **1**–**4** are 1.05×10^{-12}, 1.05×10^{-12}, 3.88×10^{-12}, and 4.27×10^{-12} esu, respectively.

The corresponding modulus of the hyperpolarizability, γ, was obtained from $|\gamma| = \chi^{(3)}/NF^4$, where N is the number density of the compound (concentration), F^4, the local field correction factor, is 3. The γ values (4.80×10^{-30} esu for **1**, 5.19×10^{-30} esu for **2**, 1.57×10^{-29} esu for **3**, and 2.04×10^{-29} esu for **4**) are larger than those observed in other ferrocenyl complexes, whose γ values range from 10^{-35} to 10^{-31} esu.[44] In general, nonlinear optical behavior governed by the nonlinear hyperpolarizability, γ, of the materials: the larger the γ value, the better the materials' NLO properties. On the other hand, from these data we can see that the γ values of the same metal ions are very close, and the γ values of **3** and **4** (Cd^{II} polymers) are a little larger than those of **1** and **2** (Pb^{II} polymers). This may be attributed to the influence of the central metal ions. The influence of these polymers' dimensionality on the third-order NLO properties is not very noticeable. Upon summarizing the limited literature relating to the third-order NLO properties of coordination polymers, we find that the coordina-

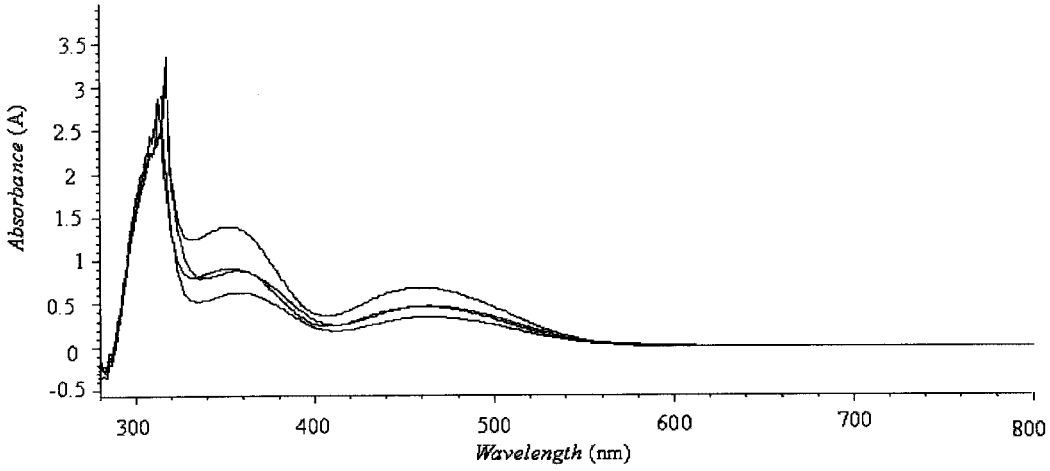

Figure 8. The UV/Vis spectra of polymers **1**–**4** in DMF solution.

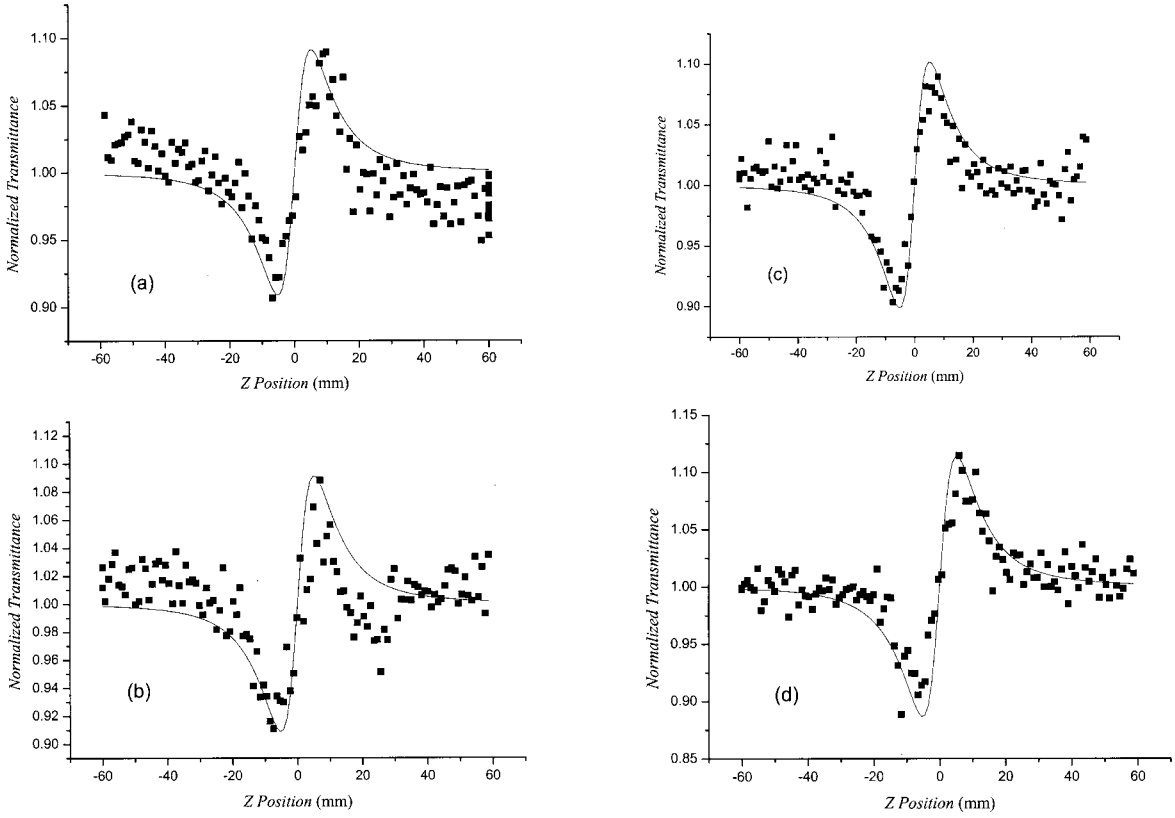

Figure 9. Z-scan data for **1**–**4**. The data were assessed by dividing the normalized Z-scan data obtained in the closed-aperture configuration by the normalized Z-scan data obtained in the open-aperture configuration. The black dots are the experimental data, and the solid curve is the theoretical fit. (a) The self-focusing effects of **1** in 1.21×10^{-4} M DMF solution at 532 nm. (b) The self-focusing effects of **2** in 1.12×10^{-4} M DMF solution at 532 nm. (c) The self-focusing effects of **3** in 1.37×10^{-4} M DMF solution at 532 nm. (d) The self-focusing effects of **4** in 1.16×10^{-4} M DMF solution at 532 nm.

tion polymers' large NLO properties may mainly be ascribed to the effect of metal ions, because the incorporation of transition metal ions into polymers can extend the π-conjugation length of the molecules, and the large π-conjugation system is favorable to increase the NLO susceptibility $\chi^{(3)}$ values.[45,46]

All the four polymers display self-focusing behavior, which is consistent with the previous conclusion[45] that the NLO properties of polymers are further controlled by the valence shell structures of the central metal ions. Nearly all the reported polymers with d^{10} valence shell metal ions give self-focusing behaviors, such as theorganic–metal polymers $[Zn(bbbt)(NCS)_2]_n$, $[Zn(pbbt)(NCS)_2]_n$,[45] $[HgI_2(4,4'\text{-azopyridine})]_n$, $[HgI_2(bpea)]_n$, $[Pb(NCS)_2(bpea)]_n$,[47] $[Cd(en)(NO_3)_2(4,4'\text{-bpy})]_n$,[48] and the ferrocenyl complexes $[Zn(4\text{-PFA})_2(NO_3)_2](H_2O)$, $[Hg_2(OAc)_4(4\text{-BPFA})_2](CH_3OH)$, $[Cd_2(OAc)_4(4\text{-BPFA})_2]$[4] etc. Other than the valence shell structures of the central metal ions, some other factors also have an effect on the intensity of the third-order optical nolinearity, such as the orbital overlap, orbital symmetry, degree of electron delocalization, linear polarizability etc. Further studies on the structure and third-order NLO properties relationship in these polymers are still underway. We believe that the study of third-order NLO properties of this kind of polymer may provide some promising candidates for the design of optical materials.

Conclusion

From the above discussion we can conclude that β-ferrocenylacrylate [FcCH=CHCOONa, Fc = $(\eta^5\text{-}C_5H_5)Fe(\eta^5\text{-}C_5H_4)$] is an excellent candidate to form extended structures whose versatile coordination modes can lead to the various and unpredictable structural geometries of different polymers. These metal–organic polymers possess good nonlinear optical refraction effects, and the metal ions play important roles in their NLO properties, because the incorporation of transition metal ions in polymers can extend the π-conjugation length of molecules, and the large π-conjugation system is favorable to increase the NLO susceptibility $\chi^{(3)}$ values.[45,46]

Experimental Section

General Details: All chemicals were of reagent grade from commercial sources and were used without further purification. β-Ferrocenylacrylic acid (FcCH=CHCOOH) was prepared according to the literature,[49] and its sodium salt was prepared by reaction with sodium methoxide. 1,1′-(1,4-Butanediyl)bis-1*H*-benzimidazole (bbbm) was prepared according to the literature.[50]

Preparation of $[Pb_6(\mu_2\text{-}OOCCH=CHFc)_2(\mu_3\text{-}OOCCH=CHFc)_2(\mu_2\text{-}\eta^2\text{-}OOCCH=CHFc)_2(\eta^2\text{-}OOCCH=CHFc)_2(\mu_4\text{-}O)_2]$ (1): FcCH=CHCOONa (27.8 mg, 0.10 mmol) in methanol (4 mL) was

added dropwise to a methanol solution (5 mL) of $Pb(OAc)_2 \cdot 3H_2O$ (38.0 mg, 0.1 mmol). The resultant pale-orange solution was allowed to stand at room temperature in the dark. Good quality red crystals were obtained several days later (yield: 6 mg, 58%). $C_{26}H_{22}Fe_2O_{4.5}Pb_{1.5}$ (828.92): calcd. C 37.67, H 2.68; found C 37.62, H 2.72. IR (KBr): $\tilde{\nu}$ = 3440 m, 3111 m, 2361 w, 1627 s, 1483 s, 1389 s, 1247 s, 818 m, 674 m, 489 m cm^{-1}.

Preparation of $[Pb(\eta^1\text{-}\mu_2\text{-}OOCCH{=}CHFc)_2(phen)]_n$ (2): Polymer **2** was prepared in a manner analogous to that used to prepare **1**, except that another kind of subsidiary ligand phen (phen = phenanthroline) (19.8 mg, 0.1 mmol) was added. The resultant red solution was allowed to stand at room temperature in the dark. Good quality red crystals were obtained after two weeks (yield: 28 mg, 62%). $C_{38}H_{30}Fe_2N_2O_4Pb$ (897.53): calcd. C 50.85, H 3.37, N 3.12; found C 50.39, H 3.56, N 3.38. IR (KBr): $\tilde{\nu}$ = 3445 m, 3094 s, 1637 s, 1540 s, 1372 s, 1244 m, 1101 m, 975 m, 846 m, 726 m, 670 m, 489 m cm^{-1}.

Preparation of $\{[Cd(\mu_2\text{-}\eta^2\text{-}OOCCH{=}CHFc)(\eta^2\text{-}OOCCH{=}CHFc)(H_2O)_2](H_2O)_4\}_n$ (3): FcCH=CHCOONa (55.6 mg, 0.2 mmol) in 3 mL of methanol was added dropwise to a 3 mL aqueous solution of $Cd(OAc)_2 \cdot 2H_2O$ (21.1 mg, 0.1 mmol). The resultant red solution was allowed to stand at room temperature in the dark. Good quality red crystals were obtained after a week (yield: 55 mg, 76%). $C_{26}H_{34}CdFe_2O_{10}$ (730.63): calcd. C 42.74, H 4.69; found C 42.68, H 4.73. IR (KBr): 3439 s, 3125 s, 2360 w, 1636 s, 1527 m, 1401 s, 1254 m, 1037 m, 815 m, 682 m, 488 m cm^{-1}.

Preparation of $\{[Cd(\eta^2\text{-}OOCCH{=}CHFc)(bbbm)_{1.5}Cl]\cdot 1.5H_2O\}_n$ (4): A methanol solution (5 mL) of bbbm (29 mg, 0.1 mmol) was added dropwise to an aqueous solution (2 mL) of $CdCl_2 \cdot 2.5H_2O$ (22.8 mg, 0.1 mmol) to give a clear solution. FcCH=CHCOONa (27.8 mg, 0.1 mmol) in 6 mL of methanol was then added dropwise to this mixture. Two weeks later good quality red crystals were obtained from the resultant red solution at room temperature in the dark (yield: 28 mg, 48%). $C_{40}H_{41}CdClFeN_6O_{3.5}$ (865.49): calcd. N 9.72, C 55.54, H 4.72; found C 55.49, H 4.72, N 9.70. IR (KBr): $\tilde{\nu}$ = 3432 s, 3114 s, 1633 s, 1541 s, 1398 s, 1252 m, 819 m, 750 m, 684 m, 491 m cm^{-1}.

X-ray Crystallography: Crystal data and experimental details for **1**–**4** are contained in Table 1. All the data were collected on a Rigaku RAXIS-IV imaging plate area detector diffractometer using graphite monochromated Mo-K_α radiation (λ = 0.71073 Å). Red, prismatic single crystals of **1**–**4** were selected and mounted on a glass fiber. The data were collected at a temperature of 291(2) K and corrected for Lorenz-polarization effects. A correction for secondary extinction was applied. The structures were solved by direct methods and expanded using Fourier techniques. The non-hydrogen atoms were refined anisotropically. Hydrogen atoms were included but not refined. The final cycle of full-matrix least-squares refinement was based on observed reflections and variable parameters. All calculations were performed using the SHELXL-97 program.[51] Selected bond lengths and bond angles are given in Table 2.

CCDC-233289, -261304, -233290, and -233291 for **1**–**4**, respectively, contain the supplementary crystallographic data for this paper. These data can be obtained free of charge from The Cambridge Crystallographic Data Center via www.ccdc.cam.ac.uk/data_request/cif.

Physical Measurements: C, H, and N analyses were carried out on a MOD 1106 analyzer. IR data were recorded on a Bruker Tensor 27 spectrophotometer with KBr pellets in the 400–4000 cm^{-1} region. TGA-DTA measurements were performed by heating the sample from 25 °C to 900 °C at a rate of 10 °C min^{-1} in air in a Perkin–Elmer DTA-7 or TGA-7 differential thermal analyzer.

Differential pulse voltammetry studies were recorded with a CHI650 electrochemical analyzer utilizing the three-electrode configuration of a Pt working electrode, a Pt auxiliary electrode, and a commercially available saturated calomel electrode as the reference electrode with a pure N_2 gas inlet and outlet. The measurements were performed in DMF solution containing tetraethylammonium perchlorate (nBu_4NClO_4) (0.1 M) as supporting electrolyte, with a

Table 1. Crystallographic data for **1**–**4**.

	1	**2**	**3**	**4**
Formula	$C_{26}H_{22}Fe_2O_{4.5}Pb_{1.5}$	$C_{38}H_{30}Fe_2N_2O_4Pb$	$C_{26}H_{34}CdFe_2O_{10}$	$C_{40}H_{41}CdClFeN_6O_{3.5}$
Mol. mass	828.92	897.53	730.63	865.49
Crystal system	triclinic	monoclinic	monoclinic	triclinic
Crystal size [mm]	0.21 × 0.20 × 0.19	0.20 × 0.18 × 0.18	0.22 × 0.20 × 0.19	0.20 × 0.20 × 0.18
Space group	$P\bar{1}$	$C2/c$	$P2_1/n$	$P\bar{1}$
a [Å]	10.315(2)	36.790(7)	10.746(2)	9.7369(19)
b [Å]	15.429(3)	10.477(2)	7.380(15)	10.200(2)
c [Å]	15.790(3)	8.2697(17)	35.632(3)	19.829(4)
α [°]	104.82(3)	90	90	102.76(3)
β [°]	97.59(3)	92.09(3)	91.13(3)	96.48(3)
γ [°]	91.65(3)	90	90	95.22(3)
V [Å^3]	2403.0(8)	3185.4(11)	2825.4(10)	1894.6(6)
D_c [Mg m^{-3}]	2.291	1.872	1.718	1.517
Z	4	4	4	2
μ [mm^{-1}]	11.700	6.216	1.813	1.062
Refl. collected/unique	6745/6745; R(int) = 0.0000	4485/2517; R(int) = 0.0867	6153/3740; R(int) = 0.0558	4320/4320; R(int) = 0.0000
Data/restraints/parameters	6745/6/599	2517/0/214	3740/0/353	4320/2/495
R[a]	0.0553	0.0754	0.0439	0.0974
R_w[b]	0.1230	0.2012	0.0679	0.2258
GOF on F^2	1.011	1.102	0.956	1.045
$\Delta\rho_{min}$ and $\Delta\rho_{max}$ [e Å^{-3}]	–2.311 and 2.006	–3.019 and 2.411	–0.635 and 0.681	–1.529 and 0.975

[a] $R_1 = \Sigma||F_o| - |F_c||/\Sigma|F_o|$. [b] $R_W = \{\Sigma[w(F_o^2 - F_c^2)^2]/\Sigma[w(F_o^2)^2]\}^{1/2}$.

Table 2. Selected bond lengths [Å] and angles [°] for **1**–**4**.[a]

1			
Pb(1)–O(9)	2.264(8)	Pb(2)–O(5)	2.610(11)
Pb(1)–O(1)	2.400(12)	Pb(2)–Pb(3)	3.687(12)
Pb(1)–O(8)#1	2.432(12)	Pb(3)–O(9)#1	2.267(9)
Pb(1)–O(2)	2.644(13)	Pb(3)–O(7)	2.473(11)
Pb(1)–O(3)	2.694(11)	Pb(3)–O(5)	2.536(13)
Pb(2)–O(9)	2.325(9)	Pb(3)–O(6)	2.597(14)
Pb(2)–O(9)#1	2.367(8)	Pb(3)–O(4)	2.607(10)
Pb(2)–O(3)#1	2.489(9)	O(8)–Pb(1)#1	2.432(12)
O(9)–Pb(3)#1	2.267(9)	O(9)–Pb(2)#1	2.367(8)
O(3)–Pb(2)#1	2.489(9)		
O(9)–Pb(1)–O(1)	81.4(4)	O(3)#1–Pb(2)–Pb(3)	99.2(2)
O(9)–Pb(1)–O(8)#1	83.1(4)	O(5)–Pb(2)–Pb(3)	43.4(3)
O(1)–Pb(1)–O(8)#1	75.7(5)	O(9)#1–Pb(3)–O(7)	76.2(3)
O(9)–Pb(1)–O(2)	76.5(3)	O(9)#1–Pb(3)–O(5)	75.2(3)
O(1)–Pb(1)–O(2)	49.7(5)	O(7)–Pb(3)–O(5)	74.7(4)
O(8)#1–Pb(1)–O(2)	123.6(4)	O(9)#1–Pb(3)–O(6)	122.7(4)
O(9)–Pb(1)–O(3)	72.8(3)	O(7)–Pb(3)–O(6)	74.1(4)
O(1)–Pb(1)–O(3)	147.3(4)	O(5)–Pb(3)–O(6)	50.2(4)
O(8)#1–Pb(1)–O(3)	81.5(4)	O(9)#1–Pb(3)–O(4)	79.6(3)
O(2)–Pb(1)–O(3)	137.2(3)	O(7)–Pb(3)–O(4)	145.1(3)
O(9)–Pb(2)–O(9)#1	74.9(3)	O(5)–Pb(3)–O(4)	75.1(4)
O(9)–Pb(2)–O(3)#1	104.5(3)	O(6)–Pb(3)–O(4)	99.2(4)
O(9)#1–Pb(2)–O(3)#1	75.1(3)	O(9)#1–Pb(3)–Pb(2)	38.2(2)
O(9)–Pb(2)–O(5)	84.1(4)	O(7)–Pb(3)–Pb(2)	52.4(2)
O(9)#1–Pb(2)–O(5)	72.2(4)	O(5)–Pb(3)–Pb(2)	45.0(3)
O(3)#1–Pb(2)–O(5)	142.6(4)	O(6)–Pb(3)–Pb(2)	85.5(3)
O(9)–Pb(2)–Pb(3)	94.5(2)	O(4)–Pb(3)–Pb(2)	93.4(2)
O(9)#1–Pb(2)–Pb(3)	36.4(2)	Pb(2)#1–O(3)–Pb(1)	97.1(3)
Pb(1)–O(9)–Pb(2)	107.7(4)	Pb(3)–O(5)–Pb(2)	91.5(4)
Pb(1)–O(9)–Pb(2)#1	114.2(3)	Pb(1)–O(9)–Pb(3)#1	110.8(3)
Pb(2)–O(9)–Pb(2)#1	105.1(3)	Pb(3)#1–O(9)–Pb(2)	113.6(3)
Pb(3)#1–O(9)–Pb(2)#1	105.4(4)		
2			
Pb(1)–O(1)#1	2.549(12)	Pb(1)–O(1)#3	2.734(12)
Pb(1)–O(1)#2	2.549(12)	Pb(1)–O(1)	2.734(12)
Pb(1)–N(1)	2.612(11)	O(1)–Pb(1)#1	2.549(11)
Pb(1)–N(1)#3	2.612(11)		
O(1)#1–Pb(1)–O(1)#2	150.3(6)	N(1)–Pb(1)–O(1)#3	90.8(4)
O(1)#1–Pb(1)–N(1)	81.1(4)	N(1)#3–Pb(1)–O(1)#3	149.1(4)
O(1)#2–Pb(1)–N(1)	73.7(4)	O(1)#1–Pb(1)–O(1)	74.7(4)
O(1)#1–Pb(1)–N(1)#	73.7(4)	O(1)#2–Pb(1)–O(1)	121.8(4)
O(1)#2–Pb(1)–N(1)#3	81.1(4)	N(1)–Pb(1)–O(1)	149.1(4)
N(1)–Pb(1)–N(1)#3	63.8(5)	N(1)#3–Pb(1)–O(1)	90.8(4)
O(1)#1–Pb(1)–O(1)#3	121.8(4)	O(1)#3–Pb(1)–O(1)	118.2(5)
O(1)#2–Pb(1)–O(1)#3	74.7(4)	Pb(1)#1–O(1)–Pb(1)	105.3(4)
3			
Cd(1)–O(1)	2.242(4)	Cd(1)–O(5)	2.395(5)
Cd(1)–O(3)	2.274(4)	Cd(1)–O(4)	2.579(4)
Cd(1)–O(6)	2.313(4)	Cd(1)–O(2)	2.580(5)
Cd(1)–O(4)#1	2.356(5)	O(4)–Cd(1)#2	2.356(5)
O(1)–Cd(1)–O(3)	142.98(17)	O(5)–Cd(1)–O(4)	71.80(15)
O(1)–Cd(1)–O(6)	92.27(16)	O(1)–Cd(1)–O(2)	53.78(15)
O(3)–Cd(1)–O(6)	124.73(15)	O(3)–Cd(1)–O(2)	89.57(15)
O(1)–Cd(1)–O(4)#1	97.51(16)	O(6)–Cd(1)–O(2)	144.52(14)
O(3)–Cd(1)–O(4)#1	84.23(15)	O(4)#1–Cd(1)–O(2)	87.27(16)
O(6)–Cd(1)–O(4)#1	87.57(16)	O(5)–Cd(1)–O(2)	93.28(17)
O(1)–Cd(1)–O(5)	80.75(17)	O(4)–Cd(1)–O(2)	136.12(15)
O(3)–Cd(1)–O(5)	98.37(15)	Cd(1)#2–O(4)–Cd(1)	139.94(19)
O(6)–Cd(1)–O(5)	90.48(17)	O(1)–Cd(1)–O(4)	150.72(17)
O(4)#1–Cd(1)–O(5)	177.34(16)	O(3)–Cd(1)–O(4)	54.13(14)
O(6)–Cd(1)–O(4)	78.25(15)	O(4)#1–Cd(1)–O(4)	109.53(6)
4			
Cd(1)–O(1)	2.273(12)	Cd(1)–O(2)	2.476(12)
Cd(1)–N(3)	2.301(14)	Cd(1)–Cl(1)	2.506(4)
Cd(1)–N(5)	2.347(12)	Cd(1)–N(1)	2.520(13)
O(1)–Cd(1)–N(3)	148.5(5)	N(3)–Cd(1)–N(1)	79.6(4)
O(1)–Cd(1)–N(5)	91.9(4)	N(5)–Cd(1)–N(1)	166.3(4)
N(3)–Cd(1)–N(5)	88.9(4)	O(2)–Cd(1)–N(1)	89.3(4)
O(1)–Cd(1)–O(2)	54.9(4)	Cl(1)–Cd(1)–N(1)	91.4(3)
N(3)–Cd(1)–O(2)	94.0(5)	N(3)–Cd(1)–Cl(1)	108.4(3)
N(5)–Cd(1)–O(2)	84.0(4)	N(5)–Cd(1)–Cl(1)	99.5(3)
O(1)–Cd(1)–Cl(1)	102.5(4)	O(2)–Cd(1)–Cl(1)	157.4(4)
O(1)–Cd(1)–N(1)	94.0(4)		

[a] Symmetry transformations used to generate equivalent atoms: for **1**: #1 $-x + 2$, $-y + 1$, $-z + 1$; for **2**: #1 $-x + 1$, $-y - 2$, $-z - 1$; #2 x, $-y - 2$, $z + 1/2$; #3 $-x + 1$, y, $-z - 1/2$; for **3**: #1 $-x + 5/2$, $y + 1/2$, $-z + 1/2$; #2 $-x + 5/2$, $y - 1/2$, $-z + 1/2$; for **4**: #1 $-x + 4$, $-y - 3$, $-z + 2$; #2 $-x + 3$, $-y - 3$, $-z + 2$; #3 $-x + 2$, $-y - 3$, $-z + 1$.

50-ms pulse width and a 20-ms sample width. The potential was scanned from +0.2 to +0.9 V at a scan rate of 20 $mV\,s^{-1}$.

A DMF solution of **1**–**4** was placed in the 1-mm quartz cuvette for NLO measurements. The nonlinear refraction was measured with linearly polarized laser light (λ = 532 nm; pulse width: 8 ns) generated from a Q-switched and frequency-doubled Nd-YAG laser. The spatial profiles of the optical pulses were nearly Gaussian. The laser beam was focused with a 25-cm focal-length focusing mirror. The radius of the beam waist was measured to be 35 ± 5 μm (half-width at $1/e^2$ maximum). The interval between the laser pulses was chosen to be about 5 s for operational convenience. The incident and transmitted pulse energies were measured simultaneously by two Laser Precision detectors (RjP-735 energy probes), which were linked to a computer by an IEEE interface. The NLO properties of the samples were manifested by moving the samples along the axis of the incident beam (Z-direction) with respect to the focal point.[43] An aperture 0.5 mm in radius was placed in front of the detector to assist the measurement of the self-focusing effect.

Caution! Although no problems were encountered in this work, perchlorate salts are potentially explosive. They should therefore be prepared in small quantities and handled with care.

Acknowledgments

The authors thank the National Natural Science Foundation of China (numbers 20001006 and 20371042), the Excellent Young Teachers Program in Higher Education Institute, and Henan Province for financial support.

[1] a) A. Togni, T. Hayashi, *Ferrocene, Homogeneous Catalysis*, in *Organic Synthesis and Materials Science*, VCH, Weinheim, **1995**; b) *Metallocenes* (Eds.: A. Togni, R. L. Haltermann), Wiley-VCH, New York, **1998**; c) N. J. Long, *Metallocenes*, Blackwell, Oxford, **1998**.

[2] a) N. J. Long, *Angew. Chem. Int. Ed. Engl.* **1995**, *34*, 21–38; b) M. Kira, T. Matsubara, H. Shinohara, M. Sisido, *Chem. Lett.* **1997**, 89–90; c) A. Nomoto, T. Moriuchi, S. Yamazaki, A. Ogawa, T. Hirao, *Chem. Commun.* **1998**, 1963–1964; d) H. Plenio, C. Aberle, *Organometallics* **1997**, *16*, 5950–5957.

[3] a) T. J. Pechham, A. J. Lough, I. Manners, *Organometallics* **1999**, *18*, 1030–1040; b) H. Fink, N. J. Long, A. J. Martin, G. Opromolla, A. J. P. White, D. J. Williams, P. Zanello, *Organometallics* **1997**, *16*, 2646–2650; c) P. D. Beer, F. Szemes, V. Balzani, C. M. Sala, M. G. B. Drew, S. W. Dent, M. Maestri, *J. Am. Chem. Soc.* **1997**, *119*, 11864–11875.

[4] G. Li, Y. L. Song, H. W. Hou, L. K. Li, Y. T. Fan, Y. Zhu, X. R. Meng, L. W. Mi, *Inorg. Chem.* **2003**, *42*, 913–920.

[5] a) S. S. Sun, D. T. Tran, O. S. Odongo, A. J. Lees, *Inorg. Chem.* **2002**, *41*, 132–135; b) J. A. Mata, S. Uriel, R. Llusar, E. Peris, *Organometallics* **2000**, *19*, 3797–3802; c) J. D. Carr, S. J. Coles, M. B. Hursthouse, M. E. Light, E. L. Munro, J. H. R. Tucker, J. Westwood, *Organometallics* **2000**, *19*, 3312–3315.

[6] a) Y. H. Liu, Y. L. Lu, H. C. Wu, J. C. Wang, K. L. Lu, *Inorg. Chem.* **2002**, *41*, 2592–2597; b) X. Lei, M. Shang, A. Patil, E. E. Wolf, T. P. Fehlner, *Inorg. Chem.* **1996**, *35*, 3217–3222; c) G. Baskar, K. Landfester, M. Antonietti, *Macromolecules* **2000**, *33*, 9228–9232; d) D. N. Hendrickson, S. M. J. Aubin, R. C. Squire, K. Folting, W. E. Streib, G. Christou, *Angew. Chem. Int. Ed. Engl.* **1995**, *34*, 887–889; e) H. W. Hou, L. K. Li, G. Li, Y. T. Fan, Y. Zhu, *Inorg. Chem.* **2003**, *42*, 3501–3508.

[7] C. Ramon, L. Concepción, M. Elies, E. Enric, *Inorg. Chem.* **1998**, *37*, 5686–5689.

[8] D. Guo, B. G. Zhang, C. Y. Duan, X. Cao, Q. J. Meng, *Dalton Trans.* **2003**, 282–284.

[9] G. L. Zheng, J. F. Ma, Z. M. Su, L. K. Yan, J. Yang, Y. Y. Li, J. F. Liu, *Angew. Chem. Int. Ed.* **2004**, *43*, 2409–2411.

[10] G. Li, H. W. Hou, L. K. Li, X. R. Meng, Y. T. Fan, Y. Zhu, *Inorg. Chem.* **2003**, *42*, 4995–5004.

[11] H. W. Hou, L. K. Li, Y. Zhu, Y. T. Fan, Y. Q. Qiao, *Inorg. Chem.* **2004**, *43*, 4767–4774.

[12] V. Chandrasekhar, S. Nagendran, S. Bansal, M. A. Kozee, D. R. Powell, *Angew. Chem. Int. Ed.* **2000**, *39*, 1833–1835.

[13] K. C. Kumara Swamy, S. Nagabrahmanandachari, K. Raghuraman, *J. Organomet. Chem.* **1999**, *587*, 132–135.

[14] X. R. Meng, G. Li, H. W. Hou, H. Y. Han, Y. T. Fan, Y. Zhu, C. X. Du, *J. Organomet. Chem.* **2003**, *679*, 153–161.

[15] a) F. A. Cotton, L. R. Fallvello, A. H. Reid, J. H. Tocher, *J. Organomet. Chem.* **1987**, *319*, 87–97; b) M. R. Churchill, Y. J. Li, D. Nalewajer, P. M. Schaber, P. M. Dorfman, *Inorg. Chem.* **1985**, *24*, 2684–2687.

[16] X. R. Meng, H. W. Hou, G. Li, B. X. Ye, T. Z. Ge, Y. T. Fan, Y. Zhu, H. Sakiyama, *J. Organomet. Chem.* **2004**, *689*, 1218–1229.

[17] R. Graziani, U. Casellato, G. Plazzogna, *J. Organomet. Chem.* **1980**, *187*, 381–690.

[18] N. Prokopuk, D. F. Shriver, *Inorg. Chem.* **1997**, *36*, 5609–5613.

[19] D. Guo, H. G. Mo, C. Y. Duan, F. Lu, Q. J. Meng, *J. Chem. Soc., Dalton Trans.* **2002**, 2593–2594.

[20] D. Guo, B. G. Zhang, C. Y. Duan, X. Cao, Q. J. Meng, *Dalton Trans.* **2003**, 515–516.

[21] H. W. Hou, G. Li, L. K. Li, Y. Zhu, X. R. Meng, Y. T. Fan, *Inorg. Chem.* **2003**, *42*, 428–435.

[22] R. D. Shannon, *Acta Crystallogr., Sect. A* **1976**, *32*, 751–767.

[23] P. R. Harrison, A. T. Steel, *J. Organomet. Chem.* **1982**, *239*, 105–113.

[24] a) D. J. Williams, S. J. Maginn, R. J. Davey, *Polyhedron* **1994**, *13*, 1683–1688; b) M. R. S. J. Foreman, M. J. Plater, J. M. S. Skakle, *J. Chem. Soc., Dalton Trans.* **2001**, 1897–1903.

[25] R. G. Bryant, V. P. Chacko, M. C. Etter, *Inorg. Chem.* **1984**, *23*, 3580–3584.

[26] Y. G. Shin, M. J. Hampden-Smith, T. T. Kodas, E. N. Duesler, *Polyhedron* **1993**, *12*, 1453–1458.

[27] a) C. Caffney, P. G. Harrision, T. J. King, *J. Chem. Soc., Chem. Commun.* **1980**, 1251–1253; b) S. Asirvatham, M. A. Khan, K. M. Nicholas, *Inorg. Chem.* **2000**, *39*, 2006–2007; c) A. M. Atria, A. Vega, M. Contreras, J. Valenzuela, E. Spodine, *Inorg. Chem.* **1999**, *38*, 5681–5685; d) Y. Yang, J. Pinkas, M. Noltemeyer, H. G. Schmidt, H. W. Roeskey, *Angew. Chem. Int. Ed.* **1999**, *38*, 664–666.

[28] a) D. C. Bradley, H. Chudzynska, D. M. Frigo, M. E. Hammond, M. B. Hursthouse, M. A. Mazid, *Polyhedron* **1990**, *9*, 719–726; b) C. S. Weinert, I. A. Guzei, A. L. Rheingold, L. R. Sita, *Organometallics* **1998**, *17*, 498–500; c) M. Cesari, *Gazz. Chim. Ital.* **1980**, *110*, 365; d) J. B. Parise, Y. Ko, *Chem. Mater.* **1994**, *6*, 718–720.

[29] a) A. Pandey, V. D. Gupta, H. Noth, *Eur. J. Inorg. Chem.* **1999**, 1291–1293; b) L. Mam, D. A. Payne, *Chem. Mater.* **1994**, *6*, 875–877; c) L. G. Hubert-Pfalzgraf, S. Daniele, R. Papiernik, M. C. Massiani, B. Septe, J. Vaissermann, J. C. Daran, *J. Mater. Chem.* **1997**, *7*, 753–762; d) J. Caruso, M. J. Hampden-Smith, E. N. Duesler, *J. Chem. Soc., Chem. Commun.* **1995**, 1041–1042.

[30] C. S. McCowan, T. L. Groy, M. T. Caudle, *Inorg. Chem.* **2002**, *41*, 1120–1127.

[31] L. H. Zhu, M. H. Zeng, B. H. Ye, X. M. Chen, *Z. Anorg. Allg. Chem.* **2004**, *630*, 952–955.

[32] A. Morsali, A. R. Mahjoub, S. J. Darzi, M. J. Soltanian, *Z. Anorg. Allg. Chem.* **2003**, *629*, 2596–2599.

[33] J. M. Harrowfield, H. Miyamae, B. W. Skelton, A. A. Soudi, A. H. White, *Aust. J. Chem.* **1996**, *49*, 1165–1170.

[34] A. R. Mahjoub, A. Morsali, *Polyhedron* **2002**, *21*, 197–203.

[35] A. K. Hall, J. M. Engelhard, A. Morsali, A. A. Soudi, A. Yanovsky, *CrystEngComm* **2000**, 13.

[36] A. Morsali, M. Payheghader, M. S. Salehi, *Z. Anorg. Allg. Chem.* **2002**, *628*, 12–14.

[37] a) R. Horikoshi, T. Mochida, H. Moriyama, *Inorg. Chem.* **2002**, *41*, 3017–3024; b) A. Ion, M. Buda, J. C. Moutet, E. Saint-Aman, G. Royal, I. Gautier-Luneau, M. Bonin, R. Ziessel, *Eur. J. Inorg. Chem.* **2002**, 1357–1366; c) C. Y. Duan, Y. P. Tian, Z. H. Liu, X. Z. You, T. C. W. Mak, *J. Organomet. Chem.* **1998**, *570*, 155–162; d) E. M. Barranco, O. Crespo, M. C. Gimeno, P. G. Jones, A. Laguna, M. D. Villacampa, *J. Organomet. Chem.* **1999**, *592*, 258–264; e) Y. M. Xu, P. Saweczko, H. B. Kraatz, *J. Organomet. Chem.* **2001**, *637*, 335–342.

[38] a) P. D. Beer, C. Blackburn, J. F. McAleer, H. Sikanyika, *Inorg. Chem.* **1990**, *29*, 378; b) J. D. Carr, S. J. Coles, M. B. Hursthouse, M. E. Light, E. L. Munro, J. H. R. Tucker, J. Westwood, *Organometallics* **2000**, *19*, 3312–3315.

[39] E. M. Barranco, O. Crespo, M. C. Gimeno, P. G. Jones, A. Laguna, C. Sarroca, *J. Chem. Soc., Dalton Trans.* **2001**, 2523–2529.

[40] a) J. T. Lin, S. S. Sun, J. J. Wu, Y. C. Liaw, K. J. Lin, *J. Organomet. Chem.* **1996**, *517*, 217–226; b) J. T. Lin, S. S. Sun, J. J. Wu, L. Lee, K. J. Lin, Y. F. Huang, *Inorg. Chem.* **1995**, *34*, 2323–2333; c) L. K. Yeung, J. E. Kim, Y. K. Chung, P. H. Rieger, D. A. Sweigart, *Organometallics* **1996**, *15*, 3891–3897; d) O. Briel, K. Sünkel, I. Krossing, H. Nöth, E. Schmälzlin, K. Meerholz, C. Bräuchle, W. Beck, *Eur. J. Inorg. Chem.* **1999**, 483–490; e) J. Mata, S. Uriel, E. Peris, R. Llusar, S. Houbrechts, A. Persoons, *J. Organomet. Chem.* **1998**, *562*, 197–202; f) I. S. Lee, Y. K. Chung, J. Mun, C. S. Yoon, *Organometallics* **1999**, *18*, 5080–5085; g) I. S. Lee, S. S. Lee, Y. K. Chung, D. Kim, N. W. Song, *Inorg. Chim. Acta* **1998**, *279*, 243–248.

[41] Y. S. Sohn, D. N. Hendrickson, H. B. Gray, *J. Am. Chem. Soc.* **1971**, *93*, 3603–3612.

[42] A. T. Armstrong, A. T. Smith, E. Elder, S. P. McGlynn, *J. Chem. Phys.* **1967**, *46*, 4321–4328.

[43] a) M. Sheik-Bahae, A. A. Said, T. H. Wei, D. J. Hagan, E. W. V. Stryland, *IEEE J. Quantum Electron.* **1990**, *26*, 760–769; b) H. W. Hou, X. Q. Xin, J. Liu, M. Q. Chen, S. Shi, *J. Chem. Soc., Dalton Trans.* **1994**, 3211–3214.

[44] a) Y. P. Tian, Z. L. Lu, X. Z. You, *Acta Chim. Sin. (Chin. Ed.)* **1999**, *57*, 1068–1072; b) S. Ghosal, M. Samoc, P. N. Prasad, J. J. Tufariello, *J. Phys. Chem.* **1990**, *94*, 2847–2851; c) Z. Yuan, G. Stringer, I. R. Jobe, D. Kreller, K. Scott, L. Koch, N. J. Taylor, T. B. Marder, *J. Organomet. Chem.* **1993**, *452*, 115–120.

[45] X. R. Meng, Y. L. Song, H. W. Hou, Y. T. Fan, G. Li, Y. Zhu, *Inorg. Chem.* **2003**, *42*, 1306–1315.

[46] a) H. W. Hou, X. R. Meng, Y. L. Song, Y. T. Fan, Y. Zhu, H. J. Lu, C. X. Du, W. H. Shao, *Inorg. Chem.* **2002**, *41*, 4068–4075; b) H. W. Hou, Y. L. Wei, Y. L. Song, Y. Zhu, L. K. Li, Y. T. Fan, *J. Mater. Chem.* **2002**, *12*, 838–843.

[47] Y. Y. Niu, Y. L. Song, T. N. Chen, Z. L. Xue, X. Q. Xin, *CrystEngComm* **2001**, 36.

[48] L. K. Li, B. Y. Chen, Y. L. Song, G. Li, H. W. Hou, Y. T. Fan, L. W. Mi, *Inorg. Chim. Acta* **2003**, *344*, 95–101.

[49] G. D. Broadhead, J. M. Osgerby, P. L. Pauson, *J. Chem. Soc.* **1958**, 650–654.

[50] X. J. Xie, G. S. Yang, L. Cheng, F. Wang, *Huaxue Shiji (Chin. Ed.)* **2000**, *22*, 222–223.

[51] G. M. Sheldrick, *SHELX-97*, Program for the Solution and Refinement of Crystal Structures, University of Göttingen, Germany, **1997**.

Received: January 22, 2005
Published Online: July 12, 2005

